Liquefaction characteristic of intermediate soil including gravel

Tadashi Hara
Kochi University, Kochi, Japan

Hirofumi Toyota & Susumu Takada
Nagaoka University of Technology, Niigata, Japan

Kouichi Nakamura
Tottori University, Tottori, Japan

SUMMARY:
Liquefaction potential evaluation is one of the most important issues in the seismic design of structures. Although a lot of research on liquefaction characteristics of sands has been carried out so far, well-graded gravelly soil has not been investigated so much in terms of liquefaction. This study investigated a coastal area reclaimed using intermediate soil including gravel. To estimate the liquefaction characteristics at several spots of reclaimed land, in-situ investigations and laboratory tests were conducted. Results revealed that, when non-plastic fines were mixed in intermediate soil, liquefaction characteristics hardly changed with different the relative density.

Keywords: Liquefaction, Intermediate soil, Gravel, In-situ test, Triaxial test

1. INTRODUCTION

The scope of problems related to the dynamics of sandy soil during earthquakes has, over recent years, expanded to include not only cases of sand with small uniformity coefficients, but also gravel and soils with fine non-plastic components. During the 1995 Southern Hyogo Prefecture earthquake, Port Island and other landfill areas experienced liquefaction that resulted in extensive damage to many buildings, despite their being on granite soil with a silt layer composed of a wide range of grain sizes including 30–60% gravel, a soil composition previously considered resistant to liquefaction (Shibata et al., 1995). Liquefaction of gravelly soil was also confirmed in the 1987 Borah Peak earthquake in the United States (Andrus, 1994) and the 1993 Hokkaido earthquake (Kokusho et al., 1994). In many cases, it is difficult to appropriately determine strength coefficients and liquefaction conditions, because soil properties may include pockets of sand, gravel, and silt with widely differing grain sizes, not only in landfill areas but also in alluvial soils. Efforts in recent years to utilize resources to the fullest extent have resulted in an increasing trend toward the use of areas with low-quality, course-grained soil, as well as demolition scrap and industrial waste as landfill (Taya et al, 2004), making understanding the conditions in which liquefaction occurs in gravel and fine-grain soils all the more important.

Recent studies related to the effects of gravel components on liquefaction strength have focused on gravel content ratios, grain composition, relative density, and the like, but there remain many unanswered questions as compared to our understanding of sandy soils (Tanaka et al., 1987 and Hara and Kokusho, 2000 and Hara et al.,2005). In contrast, numerous recent studies on the effects of plasticity index, silt composition, and clay composition have made clear the effect of fine grain content and composition on resistance to liquefaction of sandy soils (Ishihara et al., 1989 and Hwang et al., 1993 and Kuwano et al., 1995).

The present study examines intermediate landfill soils with high gravel or fine grain content, performing in situ tests to determine penetration resistance and shear wave velocity values. We also performed laboratory testing on landfill ground samples to determine their physical properties, liquefaction strength, and deformation characteristics after liquefaction. Based on these experiments, we investigate the liquefaction characteristics of intermediate soils with gravel content.

2. INVESTIGATION SITE

We selected Hirogawa Island in Wakayama Prefecture as a case of a landfill site with soil including gravel at which to perform our investigation. Figure 1 shows a map of the area. The site is at the mouth of the Hiro River, and extends approximately 500 m in the north-south direction and 250 m in the east-west direction. Land use differs along the north-south direction: On the northern side are public facilities such as the town hall, a municipal gymnasium, a health and welfare center, and a multipurpose plaza. The southern side is predominantly residential subdivisions. Construction of the landfill began in 1993 and ended in 1995, and landfill is mainly composed of cuttings from the construction of the nearby Hirogawa wind farm and drilling remains from the creation of a tunnel for the Yuasa-Gobo highway. The excavated soil is largely Mesozoic sandstone and mudstone from south of the Aritagawa river basin. Country rock has experienced weathering due to the influence of groundwater.

Figure 2 shows a geologic cross section of the area, based on boring samples taken during construction of the health and welfare center adjacent to the Hirogawa town hall, along the line indicated by A and A′ in Figure 1. According to this diagram, the landfill layer (FL) extends more or less horizontally to approximately G.L. -4.75 m, and below that are interbedded slopes of alluvial sand (As), clay (Ac), and gravel (Ag) layers sloping west until reaching the sandstone layer (Ss). Figure 2 also shows the relation between depth and *N*-values obtained by a standard penetration test. *N*-values exceed 50 in some locations due to contact with gravel, but *N* values as low as 3–10 are also seen despite an overall good grain size distribution including gravel.

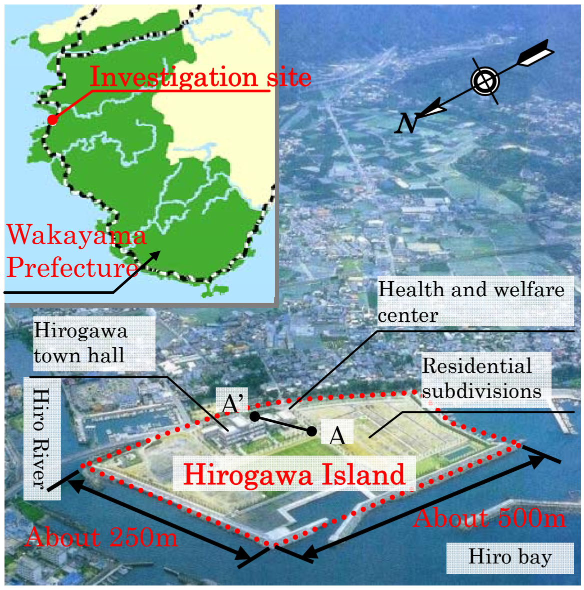

Figure 1. Location of Hirogawa Island

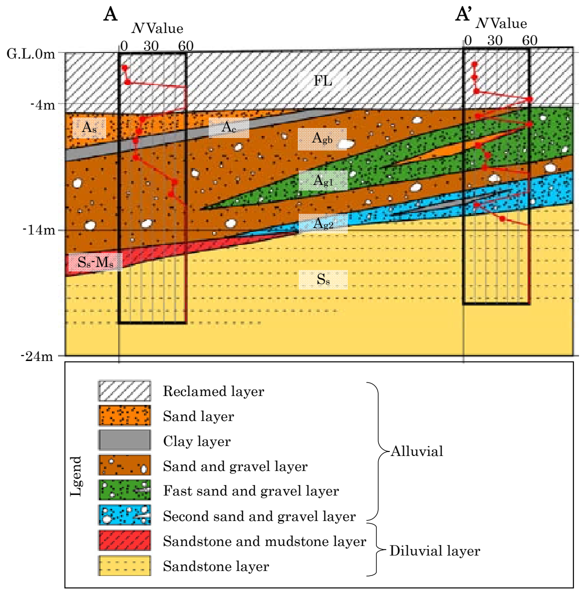

Figure 2. Geological section of Hirogawa Island

3. IN-SITU TEST ON RECLAIMED LAYER
5

To investigate hardness in the depth direction, we conducted in situ Swedish weight sounding (SWS) tests and surface wave exploration (SWE) tests (Photo 1). Figure 3 shows a map of the testing area and the locations where in situ testing was performed. SWS tests were performed mainly in the area adjacent to the seawall near the municipal multipurpose plaza, and SWE tests were performed along five north-south and east-west survey lines in the surrounding area.

Figure 4 shows an example of the relation between depth and *N*-value according to one of the SWS tests (Takada et al., 2010). Here, *N*-values are calculated according to the conversion method for gravel, sand, and sandy soils proposed by Inada. The histogram in the figure is an estimation based on insertion noise and vibration transmitted along the rod during penetration, and from soil that adhered

(a) Swedish weight sounding

(b) Surface save exploration

Photo 1. In-situ tests

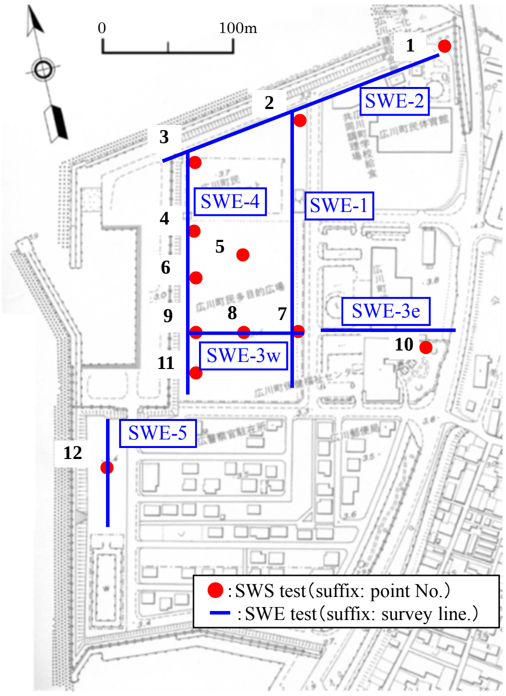

Figure 3. In-situ investigation site

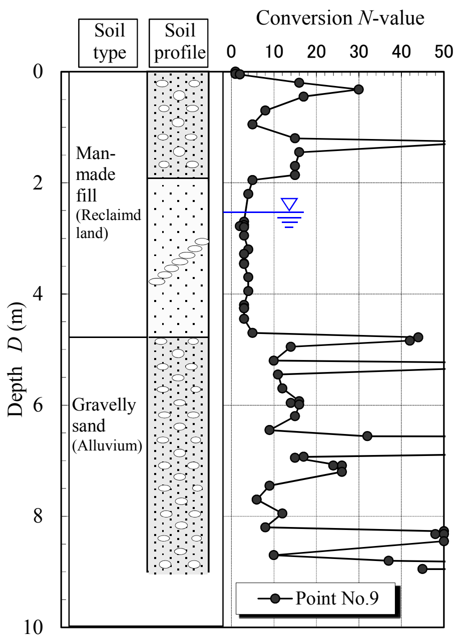

Figure 4. Soil profile at Hirogawa Island (Point No.9)

to the rod and screw. The groundwater depth (G.L. -2.6 m) is calculated from the mean value over multiple groundwater level measurements from the holes left by penetration tests. Penetration resistance values were obtained by an insertion rod contacting gravel to a depth of approximately G.L.-1.95 m, and values varied widely from N =10–50. In contrast, values below G.L. -1.95 m were an extremely loose N = 3–6, but N-values again suddenly increased below G.L. -4 m. While the test method and locations differ, results of SWS tests gave similar results to those shown in Figure 2, with a loose fill layer of approximately N = 11 in the area between G.L. -2 m and -4.5 m.

Figure 5 shows an example of the results of surface wave exploration obtained through the SWE tests performed along the SWE-3w survey line. The relation between ground depth and hardness as indicated by the magnitude of S-wave velocity fits well with Figure 2 and the N-value distribution. Namely, there is a layer of soil distributed approximately horizontally near the surface with hardness sufficient to exceed V_s = 260 m/s, but in the landfill layer below G.L. -2.5 m there is a soft layer deposit with low V_s values of 200–220 m/s, approximately the same as the mean values seen in granite soil landfill that liquefied during the Southern Hyogo Prefecture earthquake (Yamazaki et al., 1995). At depths below G.L. -4.5 m, V_s shows a clear trend of increasing with depth. While not shown in the diagram, cross-sectional surveys verified a soft layer with V_s values of 160–200 m/s at approximately

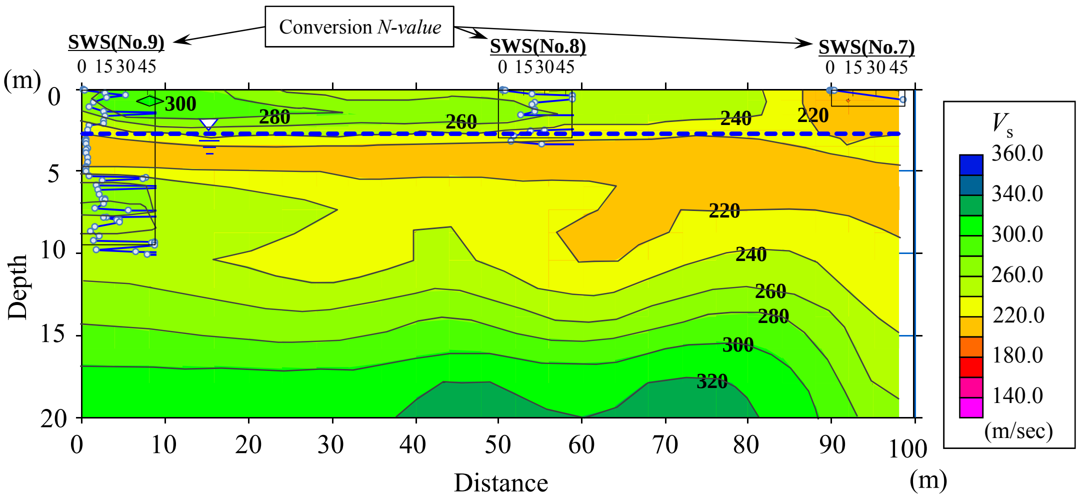

Figure 5. Surface wave exploration result (SWE-3w survey line)

G.L.-2.5 to -4.5 m horizontally along the SWE-5 survey line.

Results of the in situ testing described above indicate that the landfill layer of the soil in Hirogawa includes a soft layer with *N*-values of approximately 5 at a depth of G.L. -2 to -4.5 m, having S-wave velocities of 160–220 m/s. According to Kokusho and Yoshida, the gravelly soil in which liquefaction occurred had *N*-values of approximately 5 to 10, and S-wave velocities of 60–200 m/s. This indicates that based on in situ testing results alone, the soil in the areas tested has a high probability of experiencing liquefaction.

4. SOIL MATERIALS AND MINIMUM AND MAXIMUM DENSITY TEST

Test samples were composed of intermediate soil that included gravel with a maximum grain diameter of 26.5 mm taken from the soil used as landfill in Hirogawa ("Hirogawa soil," below). To prevent caking of the fine fraction through aggregation, disturbed samples were allowed to dry naturally for approximately one week after removal from the sampling site. Figure 6 shows a grain size distribution curve for the Hirogawa soil. There is a fairly broad range of granularity compositions in the samples, with fine grain composition F_c ranging from 0–50% and gravel composition ranging from 20–70%. After being passed through a 0.425 mm sieve, Hirogawa soil had a plasticity index Ip of 17, indicating some level of plasticity in the samples. The water absorption rate of gravel grains larger than 2 mm as determined by specific gravity and water absorption testing was a large Q = 12–20%, indicating significant porosity and extensive weathering. Rock slaking testing using the JHS 110-2006 method indicated a slaking rate R_s of 40–70%, suggesting high slaking behavior and a tendency to crumble after repeated exposure to moisture.

Figure 7 shows the relation between minimum and maximum density and fine grain content as indicated by the minimum and maximum density test apparatus shown in Figure 8. Figure 7 also shows similar relations for laboratory-prepared samples of hard alluvial gravel with differing grain sizes and undisturbed granite soil samples collected after the Southern Hyogo earthquake. The plotted values are means for 10 repetitions of the minimum density test and 5 repetitions of the maximum density test, using fine grain content equivalent to the intermediate value of the grain size distribution curve in Figure 6. From this, we can see that minimum and maximum compression of the Hirogawa soil have lower values than do alluvial gravel with large mean coefficients and granite soil with high grain fragmentation characteristics, despite differences in fine grain content.

5. TRIAXIAL TEST

We next used the cyclic triaxial test apparatus shown in Figure 9 to investigate the liquefaction

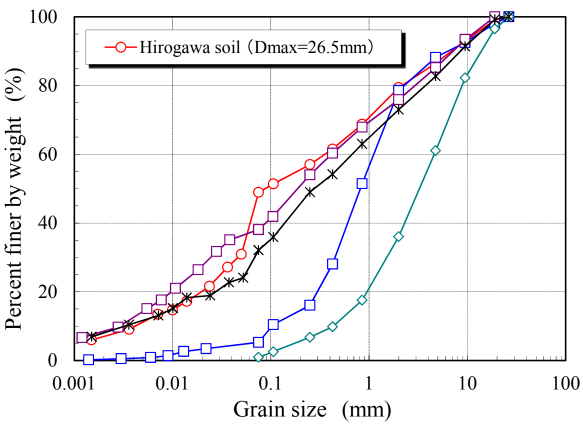

Figure 6. Grain size distribution curve for the Hirogawa soil

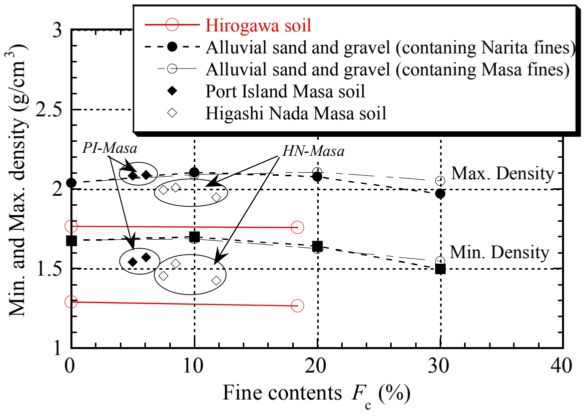

Figure 7. Minimum and Maximum density tests result for the Hirogawa soil

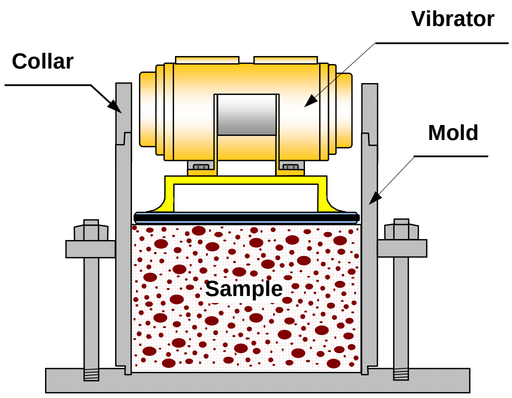

Figure 8. Minimum and Maximum density test apparatus

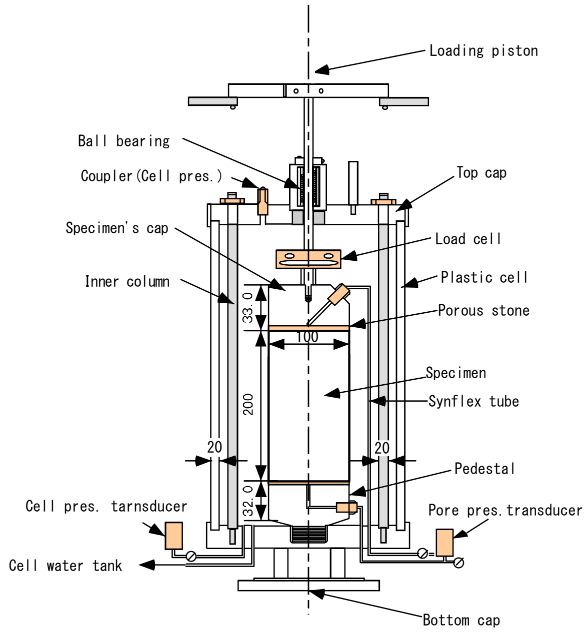

Figure 9. Cyclic triaxial test apparatus

characteristics of Hirogawa soil, and the effects of relative density and fine grain composition on its deformation after liquefaction (Hara and Kokusho, 2004). Figure 10 and Table 1 show the grain size distribution curve and the physical characteristics of the samples, respectively. Two samples were prepared in the laboratory for this test. Sample A was prepared with a grain composition of approximately the intermediate value of the grain size distribution curve in Figure 6. Sample B was prepared by washing Sample A through a 0.075 mm aperture sieve to remove the fine-grain fraction.

To minimize the influence of grain classification, the specimens were adjusted to an approximately 5% water content in separately prepared containers, then compressed into molds according to the wet tamping method using a 49 mm diameter rammer. After compression, each sample was prepared so that the relative specimen densities were $D_r \approx$ 40%, 50%, and 60%. After confirming that the pore pressure coefficient B was at least 0.96 assuming a back pressure of 98 kPa for each specimen, we applied isotropic compaction with effective confining pressure σ_c' =49 kPa, approximately equal to the effective overburden pressure on the landfill layer. Compression time was approximately 1 hour, during which we confirmed that water expulsion had completely leveled off. To confirm the overconsolidation effect on liquefaction characteristics, we used a portion of Sample A to prepare overconsolidated specimens with OCR =3.0 after pre-consolidation at the prescribed consolidation stress and drainage unloading.

Liquefaction tests were performed under undrained conditions using 0.1 Hz sine wave loads, cycled until a double amplitude axial strain DA of 5% was reached. Overall smoothness of the specimen sides

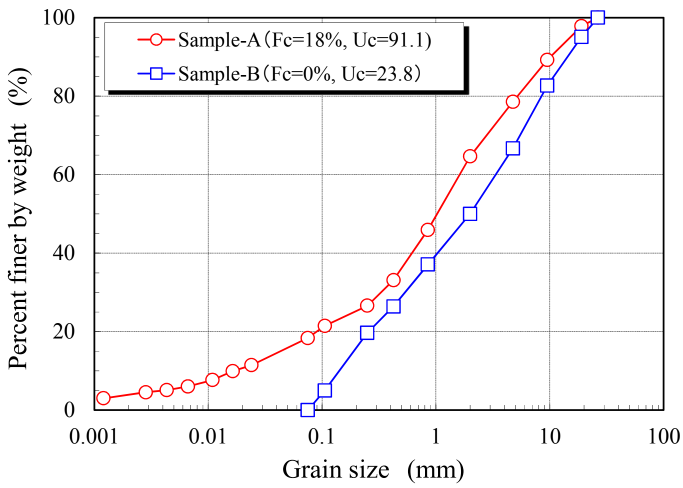

Figure 10. Grain size distribution curve for triaxial tests samples

Table 1. Physical characteristics for triaxial tests samples

Soil Material	ρ_s (g/cm^3)	ρ_{dmin} (g/cm^3)	ρ_{dmax} (g/cm^3)	e_{max}	e_{min}	I_p	D_{50}	U_c
Hirogawa soil (Sample-A)	2.736	1.758	1.263	1.166	0.556	17	1.03	91.1
Hirogawa soil (Sample-B)	2.686	1.289	1.765	1.084	0.522	NP	2.02	23.8

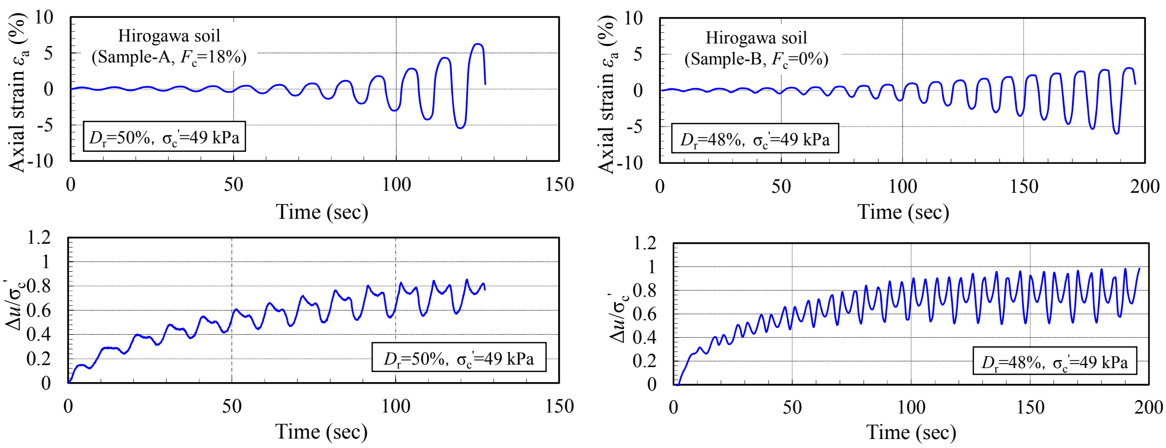

(a) Sample-A (b) Sample-B

Figure 11. Example of axial strain and excess pore water ratio time history of cyclic triaxial tests

was good, indicating little influence of membrane penetration correction.

Figure 11 shows an example of the axial strain and excess pore water ratio time history of the cyclic triaxial tests using a specimen with D_r ≈50%. For sample A (Figure 11(a)), cyclic shearing resulted in an accumulation of excess pore water pressure from the start of loading and a gradual increase in axial strain ε_a with the number of cycles, but the excess pore water pressure ratio $\Delta u/\sigma_c'$ did not reach 1.0, even after double amplitude axial strain DA reached 5%. In contrast, sample B (Figure 11(b)) exhibited a rapid increase in excess pore water pressure from the start of loading, and axial strain that

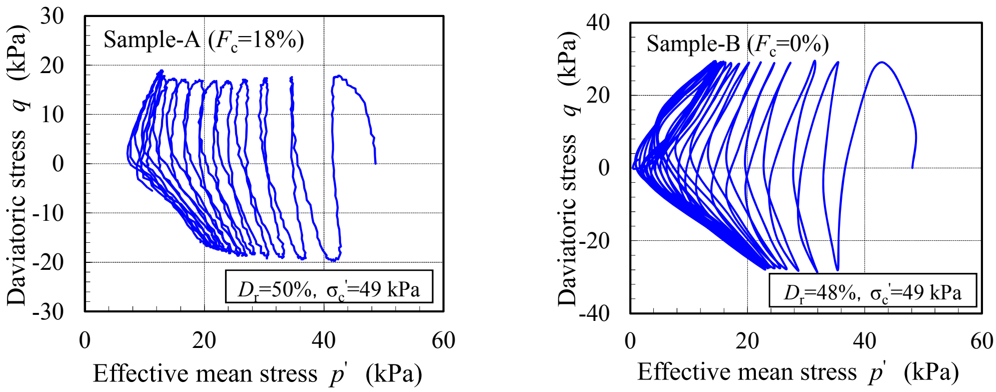

(a) Sample-A (b) Sample-B

Figure 12. Example of stress pass of cyclic triaxial tests

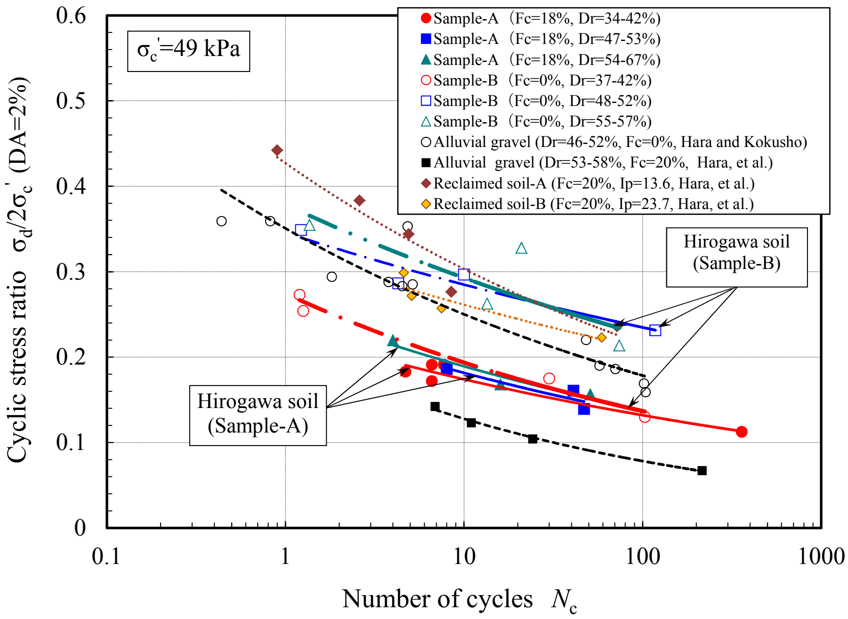

Figure 13. Undrained cyclic triaxial test results

increased with the number of cycles. Figure 12 shows the effective stress path of the results of the tests of Figure 11. Sample A shows behavior similar to loose sandy soil, where mean effective principal stress falls with the number of cycles. In contrast, Sample B indicates cyclic mobility behavior, where effective stress reduction is suppressed after reaching the phase transformation line.

Figure 13 shows the relation between the cyclic stress ratio $\sigma_d/2\sigma_c'$ and the number of cycles N_c from the undrained cyclic triaxial test when double axial strain amplitude DA reached 2%, at which necking effects are minor. Based on its plasticity index alone, the Specifications for Highway Bridges would exclude sample A from needing a determination of its susceptibility to liquefaction, but liquefaction strength R_{L20} is defined as a low 0.17 at N_c = 20 without consideration of D_r. In contrast, while the $D_r \approx$ 40% specimen from sample B has liquefaction strength similar to that of sample A, the liquefaction strength shows an overall increase with increasing relative density. Figure 13 also shows liquefaction strength curves for various alluvial sand, gravel, and landfill ground samples with plastic fine grains (Hara and Kokusho, 1998. and Hara et al., 2009). Comparing R_{L20} values, one sees that sample B has a higher strength than does sample A. This is because the gravel grain matrix is dominated by the fine-grain fraction in sample A, resulting in no change in the liquefaction strength even with an increased relative density, but in sample B, where the fine-grain fraction has been removed, sand and gravel grains are able to interlock, resulting in increased strength with higher relative density, thereby

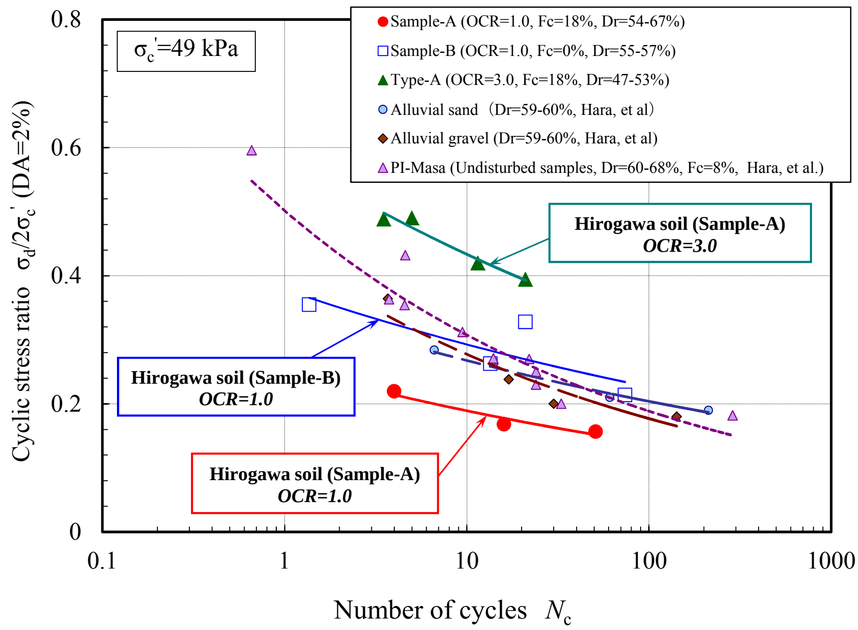

Figure 14. Undrained cyclic triaxial test results of D_r=60% the samples

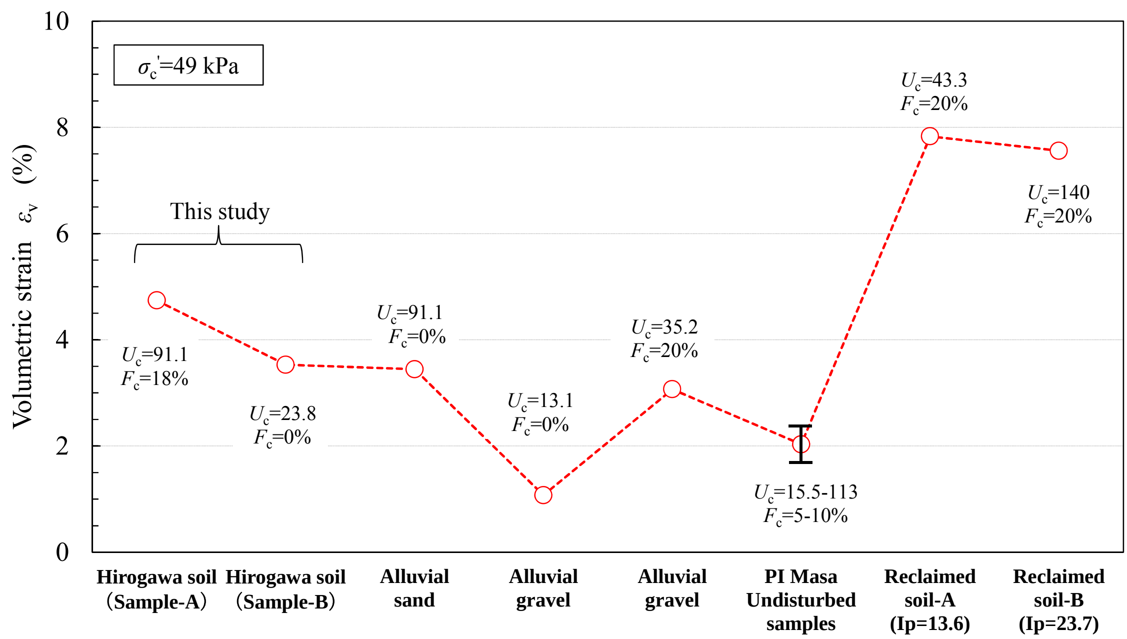

Figure 15. Consolidation test results carried out after cyclic loading

making it more like sandy gravel or clay that does not contain a fine-grain fraction. Figure 14 shows a comparison of liquefaction strengths for Hirogawa soil specimens with relative density D_r of 60% after consolidation. When the liquefaction strength of sample A, to which the overconsolidation history has been applied, is compared with that of an OCR = 1.0 sample, there is a significant increase even for those samples that include a fine-grain fraction, and the strength exceeds those of sample B and undisturbed samples of granite soil that has undergone soil stabilization treatment using rod compaction taken from Port Island.

Figure 15 shows the mean results of reconsolidation tests on a $D_r \approx 50\%$ specimen after liquefaction testing, giving volumetric strain ε_v values at an effective confining pressure σ_c' of 49 kPa. Here, volumetric strain was found immediately after removing the load when DA reached 10%, based on the amount of drained water in a burette when specimens were returned to the drained state at the point of completion of the initial consolidation before the liquefaction strength test. Variation in the amount of

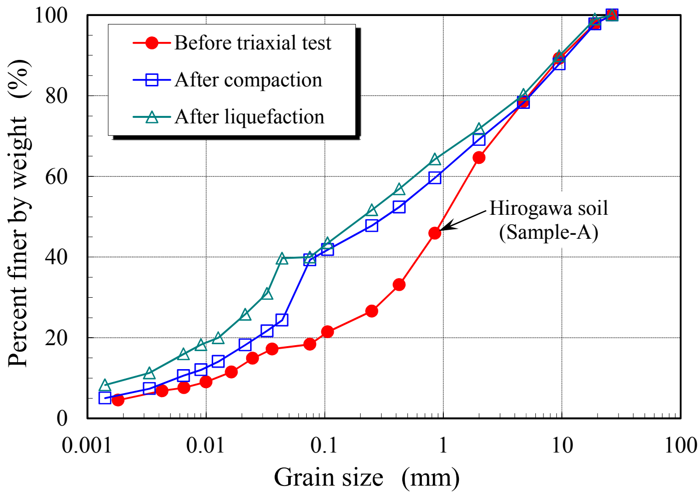

Figure 16. Comparison of grain size distribution curve

volumetric strain among the specimens was ε_v = 4.2–5.0% for sample A, and ε_v = 3.1–4.0% for sample B. Mean values for volume change associated with the dissipation of excess pore water pressure during the reconsolidation process were smaller for sample B, from which the fine-grain fraction had been removed, than for sample A. Figure 15 also shows the same relation for various D_r = 50% alluvial sand, sandy gravel, granite soil, and landfill ground samples with a plastic fine-grain fraction. The change in volume for the Hirogawa soil after liquefaction was smaller than for soils containing a plastic fine-grain fraction, but greater than for the alluvial gravel containing hard grains regardless of F_c. Values were similar to those of alluvial sand with a small mean coefficient and alluvial gravel with a non-plastic fine-grain fraction, and to granite soil with highly friable grains.

Figure 16 shows an example comparison of the grain size distribution curves for $D_r \approx 50\%$ specimens after cyclic undrained triaxial testing. Here, values in the after-compaction grain size distribution curve are the results of grain size testing of specimens disassembled immediately after their creation, and values shown for the grain size distribution curve after liquefaction testing are from specimens after cyclic shearing and reconsolidation testing. From this, we see a large shift to the left in the particle distribution after liquefaction compacting and liquefaction testing of the scope covered by the present study, indicating that compaction, reconsolidation, and shearing resulted in the destruction of mainly gravel grains larger than 2 mm. The grain destruction rate B_M (Marsal, 1967) as calculated from the grain size distribution curve was 25% immediately after compaction, and 20% after the consolidation and cyclic shearing process.

CONCLUSIONS

In situ and laboratory testing of intermediate gravelly soil (Hirogawa soil) resulted in the following major findings:

1. The *N*-value of intermediate gravelly soil from landfill ground is approximately 5 and S-wave velocity is 160–220 m/s, low values that are highly similar to gravelly soils in which liquefaction has been verified.
2. Grains in Hirogawa soil are highly porous and show extensive weathering, making them prone to slaking.
3. The liquefaction strength of Hirogawa soil varies widely according to the presence of fine grains. Removing the fine-grain fraction from samples allowed interlocking of grains, resulting in high strength.
4. Post-liquefaction consolidation characteristics were highly similar to those of loose sand, regardless of the ratio of fine grains.
5. Hirogawa soil experiences destruction of gravel grains during the process of compaction, consolidation, and cyclic shearing..

AKCNOWLEDGEMENT
The authors wish to express their gratitude those who have provided valuable assistance in the preparation of this paper. Special thanks are extended to Mr. K. Takezawa of Newjec, Inc. and Mr. I. Sirai of Ground environment, Inc., who conducted the in-situ tests.

REFERENCES

Shibata, T., Oka, F. and Ozawa, Y. (1996). Characteristics of ground deformation due to liquefaction. *Soils and Foundations Special issue on geotechnical aspects of the January 171995 Hyogoken-Nambu Earthquake*, 65-79.

Andrus, R.D. (1994). In-situ characterization of gravelly soils that liquefied in the 1993 Borah Peak earthquake. *Ph.D. Dissertation presented to the University of Texas*

Kokusho, T., Tanaka, Y., Kawai, T., Kudo, K., Suzuki, K., Tohda, S., and Abe, S. (1995). Case study of rock debris avalanche gravel liquefied during 1993 Hokkaido-Nansei-Oki earthquake. *Soils and Foundations* **35:3**, 83-95.

Taya, Y., Aoki, M., Hatanaka, M., Yasu, H. and Okahashi, M. (2004). Physical and mechanical properties of crushed concrete. *39th Japan National Conference on Geotechnical Engineering*, 601-602 (in Japanese)

Tanaka, Y., Kudo, K., Yoshida, Y. and Ikemi, M. (1987). A study on the mechanical properties of sandy gravel-Dynamic properties of reconstituted sample. *Research report No.U87019, Central Research Institute of Electric Power Industry*, abiko, Japan (in Japanese)

Hara, T. and Kokusho, T. (2000). Effect of particle gradation on liquefaction and post-liquefaction strength by means of triaxial test. *Journal of Japan Society of Civil Engineering.* **645:50**, 245-253. (in Japanese)

Hara, T., Kokusho, T. and Komiyama, Y. (2004). Undrained shear characteristics of sandy-gravel containing non-plastic fines. *Journal of Japan Society of Civil Engineering.* **785:70**, 123-132. (in Japanese)

Ishihara, K. and Koseki, J. (1989). Cyclic shear strength of fine-containing sands. *12th Int. Conf. on Soil Mechanics and Foundation Engineering*. 101-106

Hwang, D., Yanagisawa, E. and Sugano, T. (1993). Shear characteristics of silt containing sand. *Journal of Japan Society of Civil Engineering.* **463:22**, 25-33. (in Japanese)

Kuwano, J., Iimura, H., Nakazawa, H. and Sugihara, K. (1995). Liquefaction strength of sand containing kaolin, 50*th Japan Society of Civil Engineers Annual Meeting*, 506-507 (in Japanese)

Takada, S., Toyota, H., Hara, T. and Nakamura, K. (2010). Liquefaction at a housing site reclaimed using well-graded gravelly soil, *Journal of the Japanese Geotechnical Society*. **5:2**, 377-390. (in Japanese)

Inada, M. (1960). Use of Swedish Weight Sounding test results, *Tsuchi-to-Kiso*. 8:4, 13-18. (in Japanese)

Yamazaki, H., Zen, K., Sado, A. and Tachishita, T. (1995). Mechanism of damage to port facilities during 1995 Hyogo-ken Nanbu Earthquake (Part5) Liquefaction potential of reclaimed land. Technical note of the port and harbour research institutue ministry of transport, Japan. 813, 167-205

Kokusho, T. and Yoshida, Y. (1997). SPT N-value and S-wave velocity for gravelly soil with different grain size distribution. *Soils and Foundations*. **37:4**, 105-113

Hara, T. and Kokusho, T. (2004). Experiments of influencing factors on minimum and maximum density for sandy-gravel. *Journal of Japan Society of Civil Engineering.* **778:69**, 151-162. (in Japanese)

Hara, T. and Kokusho, T. (1998). Liquefaction strength of gracelly soil by means of cyclic triaxial test, *10th Japan earthquake Engineering Symposium*, 1313-1318.

Hara, T., Ueno, M., Doi, K., Toyota, H., Takada, S. and Nakamura, K. (2009), Effect of relative density on liquefaction strength of intermediate soil including gravel. *44th Japan National Conference on Geotechnical Engineering*, 289-290. (in Japanese)

Hara, T., Hatayama, A, Tange, H. and Goda, Y. (2012). Effect of gravel and fines on liquefaction strength of coarse-grained soil. *47th Japan National Conference on Geotechnical Engineering*, in press (in Japanese)

Ishihara, K. and Takatsu, H. (1979). Effects of overconsolidation and K0conditions on the liquefaction characteristics of sands. *Soils and Foundations*.**19:4**, 59-68.

Hara, T. and Kokusho, T. (2005). Effect of non-plastic fines on undrained strength characteristics of sand and sandy-gravel. *Journal of Japan Society of Earthquake Engineering.* **28:93**, 1-8. (in Japanese)

Hara, T., Kokusho, T. and Hiraoka, R. (2004). Undrained Strength of Gravelly Soils with Different Particle Gradations, *13th World Conference on Earthquake Engineering*, Paper No.144, 1-9.

Marsal, R.J. (1967). Large Scale Triaxial Test of Rockfill Materials, *Proc. ASCE*, **93:2**, 27-43.